Environmental Fluid Mechanics **1:** 3–28, 2001.

Design and Testing of a Turbulence Probe for Harsh Flows

P.A. FINDLATER[a,*], S.E. GREENHILL[b] and W.D. SCOTT[b]
[a]*Agriculture Western Australia, Geraldton, WA, Australia, 6531*
[b]*Murdoch University, Murdoch, Perth, WA, Australia, 6151*

Received 2 August 2000; accepted in revised form 5 December 2000

Abstract. The force of wind on the ground created by turbulent eddies is commonly used to describe the horizontal flux of material during wind erosion. Here we present the Murdoch Turbulence Probe, an instrument for use in both clean and eroding flows which uses pressure differences to measure the three components of wind velocity. Correlation techniques calculate the forces near the ground and turbulence statistics in nearly real time, including turbulent velocity fluctuations from less than 0.1 Hz to 200 Hz, mean flow velocities, Reynolds stresses as well as the integral length and time scales. In the portable wind-tunnel used by Agriculture Western Australia, turbulence statistics were recorded over stable surfaces and in blowing sand from the initiation of erosion up to the time the sand supply was exhausted. Estimates of the friction velocity derived from the turbulence probe were compared with estimates obtained from the wind speed profile measured with a rake of pitot and static tubes. The Murdoch Turbulence Probe appears to work well in sandblasting conditions. Relative turbulence intensities ranged from 0.11 to 0.2 and are in close agreement with values in the literature. The ratio of the turbulence to the friction velocity (3 to 3.2) is at the high end of the reported range. The Reynolds stress measurements agree closely with predictions of the threshold friction velocities of the sand and estimates from the wind speed profile with a von Kármán constant of about 0.3, lower than the commonly accepted value of 0.4. We suggest that the wind-tunnel profile represents the 'outer layer' of the boundary-layer that may best be described by a 'Wake Law' or 'Defect Law'. At about 54 mm above the surface, the friction velocity decreases from 0.64 m/s to 0.39 m/s and the mean velocity increases from 9.6 m/s to 11.6 m/s as the supply of sand is depleted. In addition to the friction velocity, other scales may be necessary to characterise the overriding effect of the wind and in extending wind-tunnel results to the field.

Key words: anemometer, logarithmic wind profile, turbulence statistics, von Kármán constant, wind erosion, wind-tunnel

1. Introduction

Wind erosion is a significant problem in Australia; we need to understand how human activities can be modified to reduce the toll on the land. This means studying the effect of different agricultural practices on wind erosion.

Field studies of erosion are valuable but difficult, since the events that cause erosion are infrequent. Currently, the only satisfactory approach is to assess soil erodibility in controlled experiments; specifically, to measure how much soil is removed in artificially imposed winds. This is most often done using wind-tunnels, but there

*Corresponding author, E-mail: pfindlater@agric.wa.gov.au

is some question about whether these tunnels simulate atmospheric conditions (Scott and Tubb, 1990; Brancatisano *et al*., 1991). Turbulence statistics, including Reynolds stresses, time and length-scales and wind speed profiles may characterise the experiments. Instruments are available to make these measurements, but none are appropriate close to the surface in the harsh, eroding environment. – Hot-wire and hot-film anemometers are not able to survive sandblasting.
– The path-lengths of sonic anemometers (typically 10 cm or more) mean they cannot be used close (3–5 cm) to a surface. They are also affected by sandblasting, acoustic noise and scattering from soil particles.
– Laser-doppler systems rely on observing particles to measure velocities. During wind erosion, measurements are confounded by saltating particles.

To address these problems, Murdoch University developed a turbulence probe that is sensitive enough to measure the detail of turbulence, yet sufficiently robust to survive and function while being sand-blasted[1] . The probe measures several stresses at a single point near the surface, and more than replaces a rake of pitot and static tubes. This article describes the design of the system and presents turbulence statistics in a harsh, wind-tunnel environment. We compare estimates of the stress from the probe and a pitot-static rake in eroding conditions.

2. Background

Soil erodibity is usually defined as the streamwise soil flux; numerous equations have been developed to describe the soil flux rate (see Greeley and Iversen, 1985, for a brief summary); most have a u_*^3 dependence. The friction velocity u_* (m/s) is estimated from the slope of the wind speed profile; above the eroding particles, the profile obeys the 'Law of the Wall'.

$$u = \frac{u_*}{\kappa} \ln\left(\frac{z-d}{z_0}\right), \tag{1}$$

u (m/s) is the mean wind; κ, von Kármán constant is dimensionless and is usually accepted as being 0.4; z (m) the height; d (m) the zero-plane displacement and z_0 (m) the roughness length. Commonly, the stress[2] is considered constant and equal to u_*^2. The wind speed profile is often measured with a rake of pitot-static tubes or cup anemometers and the erodibility of different soils or treatments are compared at the same u_* (Leys, 1991; Leys *et al*., 1996).

Initially, Bagnold (1941) reasoned that the slope of the log profile shifted upward with increased roughness; in the atmosphere the meteorological forces higher up are unaffected by the surface; the stress in the air and the u_* values remain

[1] Called the Murdoch Turbulence Probe. Limited copies of a Video are available from Bill Scott, Environmental Sciences, Murdoch University. scott@maple.murdoch.edu.au. See Scott *et al*. (1993).

[2] This is often referred to as the 'shear stress'; to avoid confusion with the wind shear, it is simply called 'stress'. The form is 'normalised' for constant density; multiplying by ρ, the air density in kg/m^3, gives the appropriate units, newtons/m^2; the familiar form of the 'shear stress' is ρu_*^2.

the same. Bagnold (1941) also found that z_0 increased with erosion; the onset of erosion corresponded to a large increase in the roughness, most likely as a result of the additional drag from the saltating particles. Importantly, Bagnold states that the value of the stress at the surface remains the same with and without erosion; only the length scale increases with erosion. In Bagnold's experiments there was sufficient supply of sand, and erosion could be considered Transport Limited[3], only u_* needs to be known to characterise the erosion by the wind.

Within the saltating cloud the profile appears to be distorted, developing a 'kink'. When and if such a 'kink' occurs, it is inappropriate to estimate u_* from the slope of the profile within the saltating cloud. McKenna-Neuman and Nickling (1994) empirically demonstrate that a $\frac{1}{2}$ power law describes the profile above and within the saltation cloud. However, Scott and Carter (1986) have shown that the effect of the 'kink' can be accounted for by taking into consideration the density of the saltation cloud; this effectively 'corrects' the pitot-static measurements. Indeed, this supports the notion that the shear, determined by the slope of the profile above the saltation cloud, extends to the surface and drives the erosion process.

Apart from Bagnold's work, it seems that u_* by itself does not characterise the wind during erosion. The steady-state formulations of erosion, Scott *et al*. (1995), show the need for at least a length scale as well; this might be z_0. Scales used to characterise such environments include the micro and integral length scales, measured from correlation measurements. Measured length scales in the atmosphere are up to 100 times higher than in a wind tunnel (Raupach *et al*., 1991; Smith, 1994).

Turbulence is also used to characterise the wind. In detailed wind-tunnel experiments, Lyles *et al*. (1971) measured the effect of stable roughness and air flow on both (1) the streamwise turbulence intensity, and (2) the ratio of the turbulence intensity to u_* as obtained from the wind profile. At any one height above the surface, the turbulence intensity was constant over a range of flow rates and strongly correlated with the surface roughness. Turbulence intensities in the 'inner-layer' ranged from about 13% over a 'smooth surface' to about 27% over a 'rough surface' covered with 24.5 mm diameter spheres. Turbulence intensities decreased to less than 2% above the boundary-layer (BL). The ratio of turbulence intensity to u_* was constant over both different wind speeds and roughness, for any one height; they obtained ratios of about 2.25, in close agreement with the results from atmospheric studies (2.2) and pipe flows (2.3) (also see Raupach *et al*., 1991; Table 2).

The Murdoch Turbulence Probe is set up to measure the integral time and length scales, Reynolds stresses (including the friction velocity) and turbulence statistics.

[3] A true Transport Limited case would be one in which the air is conveying all the eroding material it can, without limitations from the source; the converse is Supply Limited erosion.

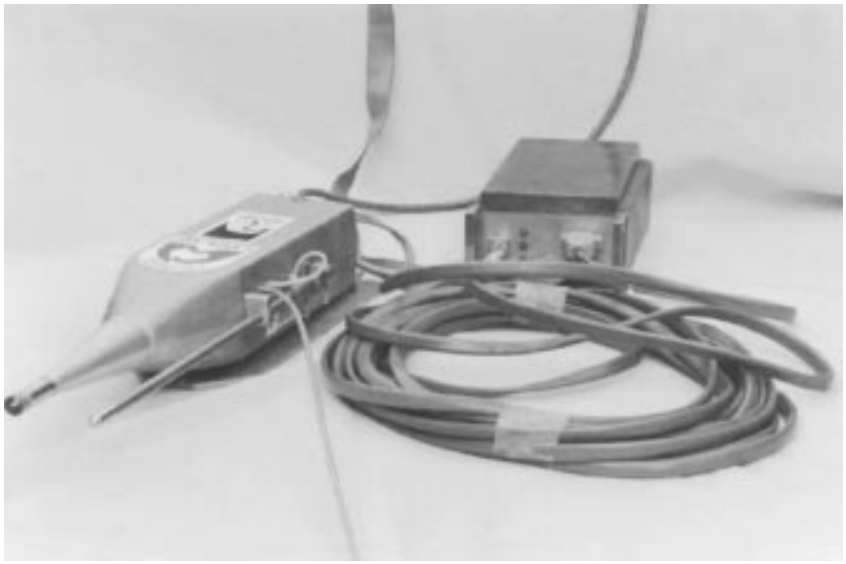

Figure 1. Murdoch Turbulence Probe system.

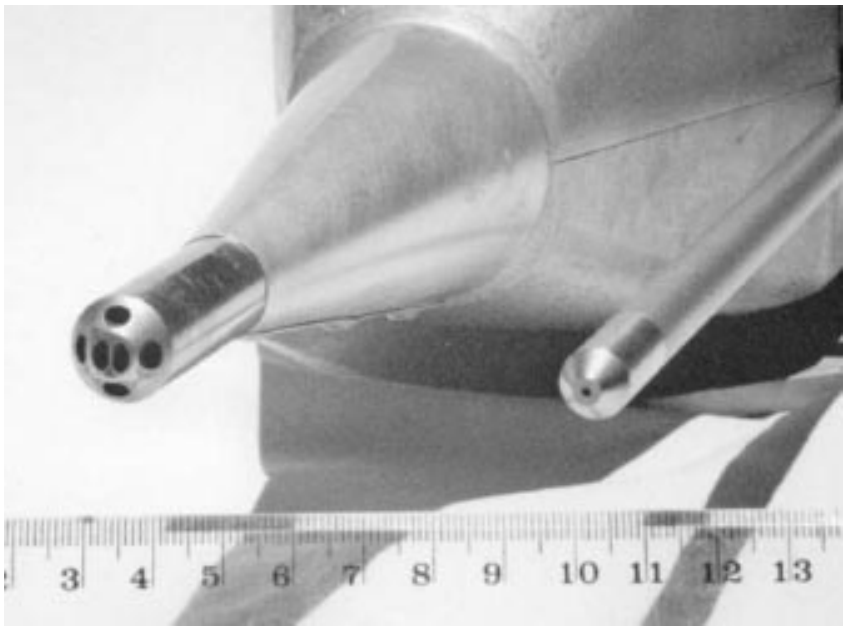

Figure 2. Detail of probe tip (*left*) and reference pitot-static tube (*right*). The scale is in centimetres.

3. Design of the Instrument

The Murdoch Turbulence Probe infers the velocity of the wind from the pressure exerted by the flow over the surface of the probe. The probe and signal processor are shown in Figure 1. The probe tip (shown enlarged in Figure 2) faces into the mean flow. Tubes transmit pressures from the surface of the probe tip to three differential pressure transducers at the rear of the probe. The transfer function of the system is carefully calibrated and digital filters are used to correct for the frequency-dependent attenuation in the tubes.

The concept of the Murdoch Turbulence Probe was based on the pressure-sphere anemometer of Wesley *et al*. (1972); this uses a 1 inch diameter sphere with 5 pressure taps to sense direction. It is clear that directional response is predicted reasonably well from potential flow theory; measured stresses over crops agree with those from a stress plate. However, as pressures are propagated down the tubes, a frequency dependent attenuation (15% attenuation at 10 Hz) and phase shift (35° at 10 Hz) occurs. Thus the pressures measured by the transducers do not correspond to the instantaneous pressures at the sensing head. This does not present a major problem in atmospheric turbulence, where the dominant scales are of the order of tens or hundreds of seconds. Over typical surfaces in wind-tunnels, however, major scales are of the order of 0.1 second and there are significant energies at higher frequencies.

Hence, several refinements of this design were incorporated into the Murdoch Turbulence Probe:

1. *Probe Tip Design*. The pressure-sphere design was found to clog rapidly in blowing sand. An alternative design uses a specially machined bundle of open tubes. This is simpler to manufacture and less prone to clogging (see Figure 2). In operation, a fine nylon screen is stretched over the head of the probe to prevent larger particles from entering the tubes. An automatic valve is also used to reverse the flow between measurements and allow compressed air to blow dust particles from the tubes.
2. *Dynamic Calibration*. Digital filters are used to correct for the transfer function of the tubing-transducer system. This gives a frequency response to at least 200 Hz.
3. *Near Real-Time Statistics*. This allows the mean wind speed, turbulence spectrum and statistics to be received directly.
4. *Realignment of Statistics*. After measurement, a coordinate rotation transforms the probe statistics to align them precisely into the mean wind. Within limits, the probe can be considered to be pointing into the mean wind, even though it may not be physically pointed into the wind[4].

[4] Algorithm worked out in detail by Scott (2001).

3.1. PROBE TIP DESIGN

Two equations were examined to explain the angular response of the probe tip. At the Reynolds numbers in use, the pressure at a point on the surface of a sphere is determined by potential flow theory (Smith, 1994, p. 47; Wesley *et al*., 1972):

$$p = p_s + \tfrac{1}{2}\rho u^2 \left(1 - \tfrac{9}{4}\sin^2\alpha\right) \tag{2}$$

where p_s (Pa) is the static pressure, ρ (kg/m^3) is the density of the fluid, u (m/s) is the fluid velocity and α is the angle between a given point and the flow axis. Note that $\alpha = 0$ at the centre point on the flow axis. Becker and Brown (1974) use a more general form to describe the response of a variety of pitot probe geometries including spherical and open-tube designs:

$$p = p_s + \tfrac{1}{2}\rho u^2 \left(1 - K\sin^{2m}\alpha\right) \tag{3}$$

where K and m are dimensionless constants determined empirically. Wind-tunnel calibration showed that the probe tip response fitted Equation (3) with $K = 1.6$ and $m = 0.65$ (Smith, 1994). The response was shown to be correct to a least 45° from the flow axis.

3.2. DYNAMIC CALIBRATION

Pressures propagated along tubing systems are affected by resonance or attenuation in the system; important considerations in wind-engineering. Wind-tunnel scale models are used to assess the likely stresses on buildings and other structures and attenuation at high frequencies allows that measured transient pressures are seriously underestimated. The same problem occurs when we measure turbulence with pressure systems. There are three approaches to dealing with tubing system transfer functions:

1. Restrict measurements to frequencies over which the transfer function is flat.
2. Modify the transfer function using restrictors and leaks.
3. Correct the signal using filters.

Where the system is largely resonant, restrictors can be inserted into the tubes to dampen oscillations. With a good model of the important factors, it is possible to evaluate alternative designs. Electrical analogies have long been used, but these are frequently inaccurate. Iberall (1950) derived a transfer function for single-ended tubing systems. Bergh and Tijdeman (1965) analysed the basic Navier-Stokes equations to give a general recursive formula for the response of a variable number of connected tubes and volumes, allowing for a flexible diaphragm in the transducer. They showed in experiments that the model can adequately describe complex systems with multiple restrictors to modify the transfer function. Further extensive studies by Holmes and Lewis (1986, 1987a) confirmed that the theory agrees closely with experimental results. Gumley (1983) extended the theory to cover simple manifolds (volumes with many input tubes) as used in wind-engineering studies for pneumatic averaging of fluctuating pressures. The extended

theory was verified experimentally by Gumley (1983) and by Holmes and Lewis (1987b).

An alternate approach is to correct the distorted pressure measurements using digital filters. Irwin *et al*. (1979) found that digital correction compared favourably to an optimal restrictor arrangement. An advantage of the technique is that it is applicable over a wider range of conditions. It can be used in highly damped (non-resonant) systems and requires only that the transfer function be measurable.

In designing the Turbulence Probe, Smith (1994) extended the analysis of Bergh and Tijdeman (1965) to care for differential pressure systems; enabling important design factors to be examined. In the Murdoch Turbulence Probe, the sensing end of the probe is separated from the transducers by about 30 cm of tubing. This allows that the flow conditions at the probe tip are not overly distorted by the relatively bulky pressure transducers. It was found that the system was highly damped: at 50 Hz, the signal level was reduced to 10% . The major damping term is scaled by (Bergh and Tijdeman, 1965)

$$\frac{n}{\pi R^2}\left(\frac{V}{k}+\xi p_s\right), \tag{4}$$

where R is the tube radius; V is the internal volume of the transducer; k and n are polytropic expansion coefficients[5] for the transducer and tube volume respectively (Smith 1994, p. 86); ξ is the diaphragm displacement per unit pressure; and p_s is the ambient atmospheric pressure. This shows that damping is increased by:

1. Reducing the tube radius,
2. Increasing the transducer volume,
3. Increasing the 'sloppiness' ξ in the diaphragm.

The theory is confirmed by experiment (Bergh and Tijdeman, 1965; Holmes and Lewis, 1986, 1987a, b; Gumley, 1983).

Here a fundamental design conflict becomes evident. The sensors need to be able to measure small velocities, of the order of 0.5 m/s. The levels of pressure involved are small (0.1 Pa, or 0.01 mm H_20), and require a very sensitive pressure transducer. For small pressures, diaphragm displacement per unit pressure or 'sloppiness' ξ needs to be maximised; for high frequencies, ξ needs to be minimised. The current design balances these factors and is sensitive up to about 200 Hz.

4. Definition of Measurements

In the wind-tunnel, the x-axis is aligned with the length of the tunnel. The y-axis is lateral to the flow, parallel to the surface and perpendicular to the flow; the z-axis is vertical and perpendicular to the surface. The components of the wind velocity are u (longitudinal), v (lateral) and w (vertical).

[5] k and n are the exponents in a power law relating pressure to density, polytropic constants. They characterise the conditions that occur during expansion in the transducer and tube, respectively. k is constant and n is a function of frequency (Bergh and Tijdeman, 1965).

It is usual to consider the longitudinal velocity u to be composed of a mean component $\bar{u}$ and a fluctuating component u'.

$$u = \bar{u} + u'. \tag{5}$$

There are similar expressions for the v and w components. Extending this statistical definition to the Navier-Stokes equations gives rise to the Reynolds stress terms, representing the stresses within the fluid due to turbulence. The Reynolds stresses are computed by taking correlations over time between components of velocity at a point in space.

In wind-erosion the following properties of the flow are of concern:

1. The wind velocity and direction ($\bar{u}$, $\bar{v}$, $\bar{w}$).
2. The turbulence intensity (absolute, $\sqrt{\overline{u'u'}}$ and relative, $\sqrt{\overline{u'u'}}/\overline{u}$), a measure of the size of the fluctuations from the mean. Here we also use $\overline{u'u'}$ as a measure of turbulence.
3. The Reynolds stress close to the surface ($-\rho\overline{u'w'}$), a measure of the force on the ground. Presuming that the fluid is incompressible the density is ignored and Reynolds stress is commonly defined as $\overline{u'w'}$ and close to the surface $u_* = \sqrt{-\overline{u'w'}}$.
4. The integral scale in time (T) and space (Λ), a measure of the size of the dominant eddies.

Correlations between velocities at different points in time can tell us about the temporal structures in the turbulence. The Eulerian time autocorrelation coefficient is defined as

$$R(\tau) = \frac{\overline{u'(t)u'(t+\tau)}}{\sqrt{\overline{u'u'}(t)}\sqrt{\overline{u'u'}(t+\tau)}}, \tag{6}$$

where τ represents the time lag. The integral time scale T is defined as the area under the curve $R(\tau)$ from $\tau = 0$ to ∞. It is not possible to measure this area but, if the flow contains no periodic components, R will eventually decrease to zero so we can use the approximation

$$T = \int_{\tau=0}^{R\approx 0} R(\tau)\mathrm{d}\tau, \tag{7}$$

T is a measure of the time scale of eddies in the flow. If Taylor's Hypothesis[6] holds, the temporal and spatial scales are related

$$\Lambda = \bar{u}T, \tag{8}$$

where Λ is the integral length scale.

[6]If a turbulent eddy is stable long enough to pass unchanged past a sensor, spatial variations in the fluid properties due to the eddy will appear as temporal variations to the sensor (see Stull, 1988, p. 5).

Figure 3. Turbulence probe trials with the AWA wind-tunnel over a 'peg-board' surface.

5. Turbulence Probe Trials

The probe evolved with two different heads, a spherical design (following Wesley *et al*., 1972) and a CETIAT[7] design (following Ower and Pankhurst, 1966, see Figures 1 and 2). The heads, and their associated electronics were trialed extensively in laminar and turbulent wind tunnels. The trials were conducted in the laminar wind tunnel at Curtin University, Department of Mechanical Engineering, and began with the five-port spherical design of Wesley *et al*., but revealed the superiority of the CETIAT Design, its response at large angles. Turbulent tests were completed in the Agricultural Wind Tunnel of Agriculture WA. Initial trials were over known surfaces, emphasising surfaces with roughness similar to what might be expected during wind erosion, Peg-board; but bitumen surfaces were included. Later, trials were conducted on eroding surfaces. All the trials were run, as possible, with side-by-side comparisons with a sensitive, high-response, dual, hot-wire system, compatible with the electronics of the Turbulence Probe. The details of calibration and trials are presented in Smith (1994).

Figure 3 shows early trials with the Mark I turbulence probe (spherical design) in the AWA[8] portable wind-tunnel at Geraldton, WA. In March 1993, the wind-tunnel was set up at Murdoch University to trial the performance of the Mark I

[7] See ISO standard 3966, 'Measurement of fluid flow in closed conduits'. Smith (1994) has design drawings. Bryer and Pankhurst (1971) and Ower and Pankhurst (1966) are the classic references to such pitot designs.

[8] Agriculture Western Australia, formerly Western Australian Department of Agriculture.

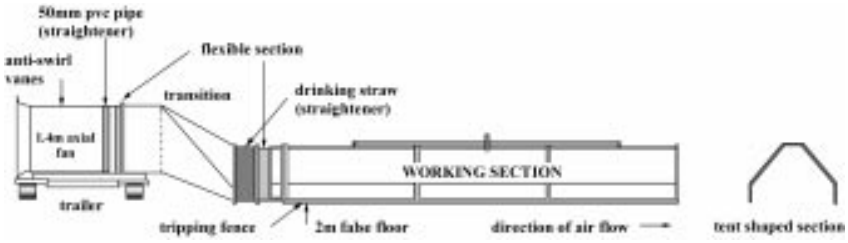

Figure 4. AWA wind-tunnel with a tent shaped cross-section. The working section following the false floor is 5.1 m long by 1.5 m wide by 1050 m high.

Murdoch Turbulence Probe in both a clean environment and during wind erosion. In a clean environment the results from the turbulence probe were well correlated with statistics obtained from a X-wire probe with correlations (r) for $\overline{u} = 0.996$, $-\overline{u'w'} = 0.962$, $T = 0.92$ and $\Lambda = 0.71$ (from Smith, 1994, Table 6.2). In eroding conditions the trials indicated that the dynamic behaviour of the eroding soil was different from the behaviour of a stable surface. The turbulence spectrum was significantly different at high frequencies. The results were reported by Smith (1994), but were inconclusive for several reasons:

1. The number of trials was small.
2. The probe was rapidly filled with sand, which may have affected the response.
3. The source material (the eroding soil surface) was rapidly depleted over the course of an experiment, and the statistics were unlikely to be stationary.

In 1994, a further study was conducted during which:

1. Modifications were done to the probe to eliminate blockage during erosion. This includes nylon screens and a flushing mechanism, as described in Section 3.1.
2. Changes were made to the data analysis procedures to deal with non-stationary statistics.
3. The pressure transducer in the Mark II version used specially-formed stainless steel diaphragms, replacing the Mylar diaphragms in the Mark I version which tended to have a variable sloppiness ξ.

6. Tests in Blowing Sand

Subsequent trials in the AWA tunnel at Albany showed that the system could be kept free of blockage if flushed every 15 s. Measurements of 15 s appeared long enough to give repeatable statistics, though less than ideal[9]. Turbulence measurements were made over stable surfaces (Peg-board, Bitumen, and Stable Sand) as well as eroding sand.

[9] 1 minute or more is preferable. It is possible to run the probe for minutes, with 15 seconds on, a few seconds off, but this complicates the statistics.

6.1. ROUGHNESS CONSIDERATIONS

The tunnel (Figure 3 and Figure 4) was set up over a bitumen surface to test if the profile parameters, particularly the vertical stress $\overline{u'w'}$ and von Kármán constant κ, are affected by erosion. Tests were over rough surfaces, as might be expected during erosion; the tests were carried out over a Peg-board surface, designed to have a silhouette density (or aspect ratio) similar to that of surface E from Raupach *et al*. (1980). The silhouette density λ is the height h, times the width divided by the separation distance squared. Surface *E* consisted of a regular array of cylinders 6 mm high of 6 mm diameter spaced 20 mm apart giving a silhouette density $\lambda = 0.09$. Over a range of scales covering several orders of magnitude and three dimensional roughness elements, Raupach *et al*. (1980) found that

$$z_0/h = \lambda \quad \text{for } (z_0/h) < (z_0/h)_{\max}. \tag{9}$$

In the same paper d was estimated for five surfaces with different element densities (Raupach *et al*., 1980, Table 1). Using these estimates we obtained an empirical regression equation.

$$d/h = 0.24\ln(\lambda) + 1.246, \quad r^2 = 0.999. \tag{10}$$

The construction of a surface with a silhouette density of 0.09, used cylinders 9.6 mm high by 9.6 mm diameter with a separation distance of 32 mm. However, after repeatedly storing and transporting the panels over 1000 km distances, it was found that the average cylinders in the Peg-board had a height h of 8 mm and a width (diameter) of 9.6, giving $\lambda = 0.075$. Using (9), $z_0 = 0.6$ mm for the Peg-board surface. This estimate of z_0 is consistent with the theory of Raupach (1992)[10].

The results over these 'stable' surfaces show that the velocity profile was 'logarithmic' over much of the tunnel but the depth of the boundary-layer was shallow – around 300 mm over a rough surface (Peg-board) and about 60 mm over a smooth surface (bitumen). Over the Peg-board the roughness length obtained from the logarithmic profile was 0.64 mm, with the zero-plane displacement of 5 mm estimated from 6.2.

When values of $\overline{u'w'}$ measured with the Murdoch Turbulence Probe were used with regression estimates of the slope of the logarithmic velocity profiles, $\kappa \cong 0.3$.

In these experiments the 'rough' surface exhibited a higher stress (friction velocity) and higher velocities above the boundary-layer than 'smooth' surface at the same engine speed. This is consistent with the measurements of Zingg and Woodruff (1951) that show the stresses increasing with increases in roughness when the velocity above the boundary is held constant. It is expected that a 'rougher' eroding surface, caused by the saltating particles, will increase the stress, contrasting with Bagnold's (1941) reasoning that the stress does not change.

[10]Raupach (1992) used a physical model to predict z_0; it applies when the width of roughness elements differs from the height and may be used to predict z_0 and d.

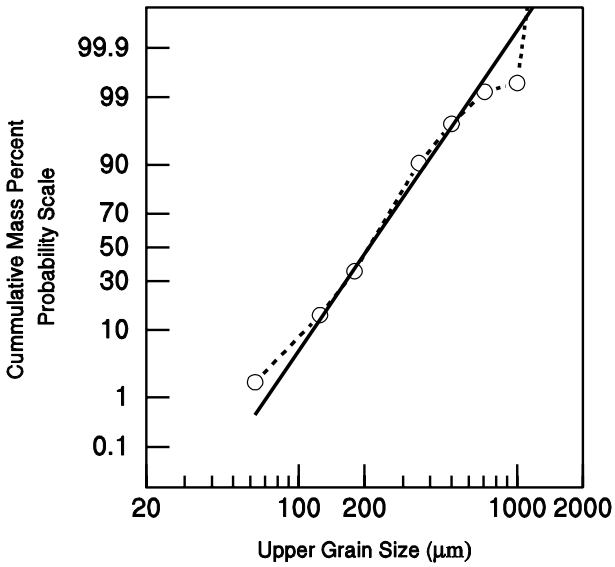

Figure 5. Distribution of sand used in tests (data from Table I). Solid line fits a log-normal distribution.

Table I. Particle size analysis of the sand. The distribution is approximated by a log-normal distribution (Figure 5) with mean 2.32 (210 μm) and standard deviation 0.2 (+124 μm, −78 μm). The fraction > 2000 μm was removed. Sample size 402.7 g.

Size μm	1000	710	500	355	180	125	63	0	Total
G	2.2	1.0	8.0	27.4	220.8	84.1	51.8	7.4	402.7
% >	0.5	0.2	2.0	6.8	54.8	20.9	12.9	1.8	100

6.2. METHOD

Sixty-five kilograms of sand (Table I and Figure 5. present the mass-size distribution) was spread evenly over the floor of the working section of the tunnel (Figures 3 and 4). A modified Fryrear trap (Shao *et al.*, 1993) with dimensions 50 cm × 20 mm was placed at $y = -165$ mm with the mid point at $z = 100$ mm. The probe was at $y = +150$ mm and $z = 54$ mm above the sand surface. Instruments were placed at the tunnel outlet and coordinates were measured with left negative and right positive, facing into the flow.

Instantaneous profiles of the mean velocity were made with a rake of pitot and static tubes placed on the centre-line ($y = 0$) with the bottom pitot at $z = 15$ mm above the sand surface. The Rake, coupled to a multi-tube inclined manometer, is mounted on a 20 mm square bar extending over the depth of the tunnel. Com-

plementary pairs of pitot (measuring total pressure) and static tubes 120 mm long are arranged logarithmically along the bar, as spacing allowed, with fewer static tubes near the surface. The stainless steel pitot tubes had an internal diameter of 2 mm and an outside diameter of 3.2 mm. The pitot tubes were open ended and cut square; the static tube was formed from a 3 mm diameter port drilled in the side of a blind tube, set 15 mm from the leading edge of the tube[11]. The pitot and static tubes are coupled to the multi-tube manometer with 6 mm PVC beverage tubing.

The multi-tube manometer is made from thirty, 1 m long glass tubes (channels) with an internal diameter of 4 mm. The glass tubes were thoroughly cleaned and connected via copper tubing at one end to a common well (negative port) containing liquid, alcohol coloured with a red dye (Oil Red O). The well is raised or lowered to adjust the level of the liquid in the manometer. The other end of the glass tube acts as the positive port.

The pitot and static tubes on the rake were connected to the positive ports of the manometer and the well is left open to atmospheric pressure. The dynamic pressure is then the difference between the pitot and the nearest static tube.

The measurements are recorded by a video camera mounted above the manometer; the image is processed using a frame grabber and software written for the purpose; it measures the height of the fluid in each tube. The video camera and manometer are enclosed in a hood and fitted with a fluorescent light to control the level of lighting.

Before each set of measurements the system is calibrated. The computer first records the position of the fluid in each tube. A known pressure, measured with a Magnehelic® gauge[12], is then applied to one of the channels. This produces a scale factor and adjusts for the incline of the manometer. During each run one channel is left open to the atmosphere to act as a zero to monitor and correct for changes in atmospheric pressure. Pressures for all tubes are recorded every 6 seconds to within 1 pascal.

The initial engine speed was set at 800 rpm, just below the threshold, to measure the surface roughness of the non-eroding surface. Then, the engine speed was increased to 1600 rpm and the wind profile was sampled until all the soil had blown away (after 2 min 30 s); 153.6 g were collected in the trap. The profile was then measured over the exposed bitumen surface with the engine speed still set at 1600 rpm. This determined (i) which pitot tubes in the Rake had become blocked, and (ii) the zero-plane displacement (d) which increased continuously during the experiment. The erosion profiles were compared with the profiles over the bitumen surface and Peg-board.

The wind velocity profile was used to obtain profile parameters including boundary-layer height δ, κ, and z_0 and their standard errors (s_i). The boundary-layer

[11]This accords with standard static tube design with the static port 5 or 6 tube-diameters aft of the base of the nose (Ower and Pankhurst, 1966). The supporting bar was relatively large to stop flexing in high winds.

[12]Dwyer Instruments, Inc., Michigan City, Indiana. USA.

height δ, was identified by the position at which the normalised profiles coincide and inflections occur in the log profiles. Estimates of δ for the sand and bitumen surfaces are far less precise than for the rougher surfaces (eroding sand and Pegboard) and may underestimate the boundary by several centimetres. Wind speed measurements at levels below δ were fitted to a logarithmic profile with a standard regression form,

$$y = ax + b, \tag{11}$$

Where y is the wind speed, x is the *ln* of the height, the slope is a and the intercept is b. Values for κ were estimated from Reynolds stress measurements and the slope of the logarithmic velocity profile; z_0 is estimated directly from the intercept. Following the log profile, Equation (1), the relations are:

$$\kappa = \frac{u_*}{a}, \tag{12}$$

and

$$z_0 = e^{(-b/a)}. \tag{13}$$

Standard errors (s) for κ, z_0 and $\ln z_0$ were estimated from the standard errors of the profile coefficients a and b using Wilkinson's (1984) procedure for estimating the confidence limits. The standard error of $f(r_1, r_2, \ldots)$, is given

$$s_f^2 = \left(\frac{\partial f}{\partial r_1}\right)^2 s_1^2 + \left(\frac{\partial f}{\partial r_2}\right)^2 s_2^2 + \ldots, \tag{14}$$

where $s_1, s_2, \ldots$ are the standard errors of $r_1, r_2, \ldots$ to first order. From this a value of the standard error for κ may be obtained. Presuming u_* is measured without error, the quantity

$$s_\kappa = \frac{u_*}{a^2} s_a \tag{15}$$

is an estimate of the standard error of κ. Here we present alternatives to Wilkinson's (1984) expressions for s_{z_0} and $s_{\ln z_0}$,

$$s_{\ln(z_0)} = \frac{s_a}{a}\sqrt{\left(\left(\frac{s_b}{s_a}\right)^2 + (\ln z_0)\right)}, \tag{16}$$

$$s_{z_0} = z_0 s_{\ln(z_0)}. \tag{17}$$

Both have the same number of degrees of freedom, two less than the number of measurements.

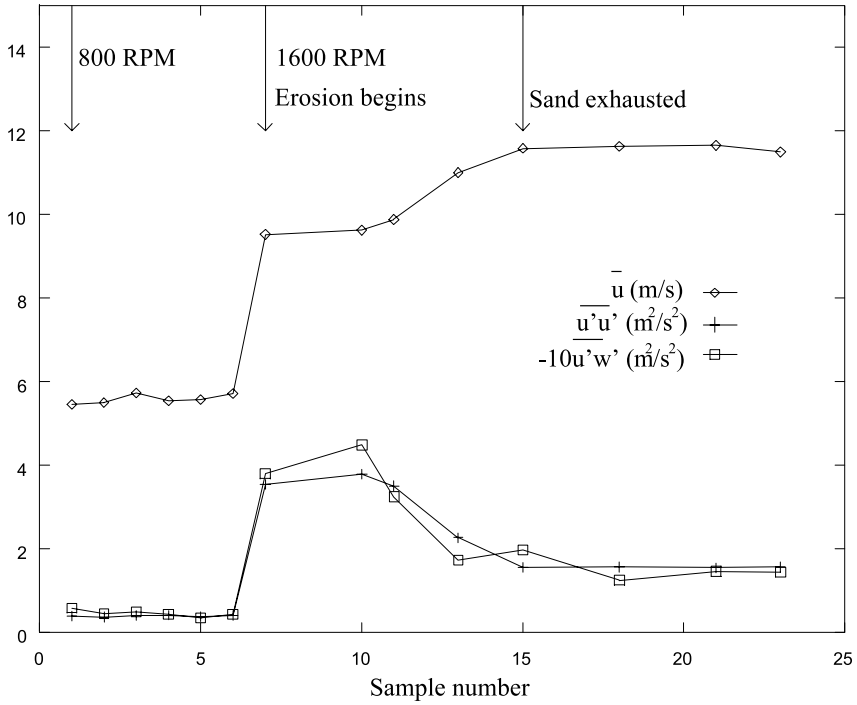

Figure 6. Mean velocity and turbulence levels during erosion.

We tested for significant differences ($P < 5\%$) between κ for each profile and the value obtained over the Peg-board. Presuming the population variances are equal, we employed a two tailed t-test.

$$t = \frac{x_1 - x_2}{\sqrt{s_1^2 + s_2^2}}. \tag{18}$$

The denominator is the pooled standard error and the degrees of freedom are summed. The t-test was also applied to the other coefficients to estimate their confidence limits.

7. Results

7.1. TURBULENCE STATISTICS

Figure 6 shows the results of a typical experiment; Table II shows statistics collected with the Murdoch Turbulence Probe averaged during different phases of the erosion process, (i) Stable Sand, (ii) Transport Limited, (iii) Supply Limited, and (iv) Sand Exhausted. The graph shows the values of the mean velocity $\bar{u}$, the

variance or turbulence $\overline{u'u'}$ and the vertical Reynolds stress $-\overline{u'w'}$ as the experiment progressed. Initially at 800 RPM the velocity and turbulence levels are low (5.5 m/s, 0.39 m^2/s^2). The stress is 0.058 m^2/s^2 ($u_* = 0.24$ m/s) and the surface is stable.

The engine speed is then changed to 1600 RPM. The wind velocity and turbulence increase (to 9.5 m/s and 3.5 m^2/s^2). The stress rises to 0.38 m^2/s^2 ($u_* = 0.62$ m/s) and the surface begins to erode. After about a minute (Figure 6, sample number 13), sufficient sand has blown away to expose the bitumen. The velocity begins to increase and the turbulence and stress decrease. After another minute (Figure 6, sample number 15) only the bitumen remains; the velocity increases to about 11.6 m/s, the turbulence and stress drop, respectively, to about 0.016 m^2/s^2 and 0.20 m^2/s^2 ($u_* = 0.44$ m/s). The velocity, turbulence and stress remain at about these levels until the end of the experiment. The magnitude of the vertical stress is approximately one tenth $\overline{u'u'}$.

The relative turbulence intensity, $\sqrt{\overline{u'u'}}/\bar{u}$, at 800 RPM was 0.11 (Table II). It increased to 0.2 during erosion and dropped to 0.11 when only the smooth bitumen surface remained. The ratio $\sqrt{\overline{u'u'}}/-\overline{u'w'}$ remained constant between 3 and 3.2. The relative turbulence intensity values are consistent with those reported by Lyles *et al*. (1971). However, $\sqrt{\overline{u'u'}}/-\overline{u'w'} \cong \sqrt{\overline{u'u'}}\Big/u_*$ is at the high end of the range of values reported in the literature (Lyles *et al*., 1971; Raupach *et al*., 1991).

These trials differ from earlier trials (see Section 5) in that the instrument, being self-cleaning, does not suffer blockage despite long periods in sandblasting conditions; artifacts previously noticed at high frequencies were absent. Figure 7 compares the autocorrelation measurements over stable sand, eroding sand (Transport and Supply Limited) and the Sand Exhausted (bitumen) case. Each curve represents an average over 4, 15-s samples. The integral time scales T (the area beneath the autocorrelation curves) are 0.041 (Stable Sand), 0.025 (Eroding Sand), and 0.017 (Sand Exhausted - Bitumen) seconds. Measurements taken over stable sand were below the threshold for erosion at low wind speeds and T is high.

7.2. PROFILE MEASUREMENTS

Two velocity profiles over the sand and two profiles over a bitumen surface are shown in Figure 8. The profile for preliminary tests without sand (dashed line) is similar to the profile over the bitumen surface immediately following the removal of sand by the wind (solid line, Sand Exhausted exposing the bitumen surface). The low velocity profile is over the sand surface prior to erosion (solid diamonds, Stable Sand below threshold for erosion). The profile during erosion (solid circles, Transport Limited case) exhibits both higher velocities but also a markedly different slope, corresponding to a much larger u_*. The profile parameters are given in Tables II and III.

Table II. Profile parameters estimated with the Turbulence Probe averaged over a number of samples (Figure 6) at each phase of erosion. ($y = -150$ mm)

Surface	Engine Speed	Sample No's.	z[a] mm	u_z m/s	T s	Λ m	$\overline{u'w'}$ m^2/s^2	$\overline{u'u'}$ m^2/s^2	$\sqrt{\overline{u'u'}}/\overline{u}$	$\sqrt{\overline{u'u'}}/-\overline{u'w'}$	u_* at z m/s
Stable sand	800	1–6	54	5.58	0.040	0.220	0.044	0.4	0.11	3.0	0.21
Transport limited	1600	7, 10	54	9.57	0.030	0.289	0.410	3.67	0.20	3.0	0.64
Supply limited	1600	11, 13		10.44	0.021	0.216	0.240	2.88	0.20	3.1	0.49
Sand exhausted	1600	15, 18, 21, 23	59	11.57	0.017	0.192	0.152	1.56	0.11	3.2	0.39

[a]Estimated height of probe relative to sand or bitumen surface.

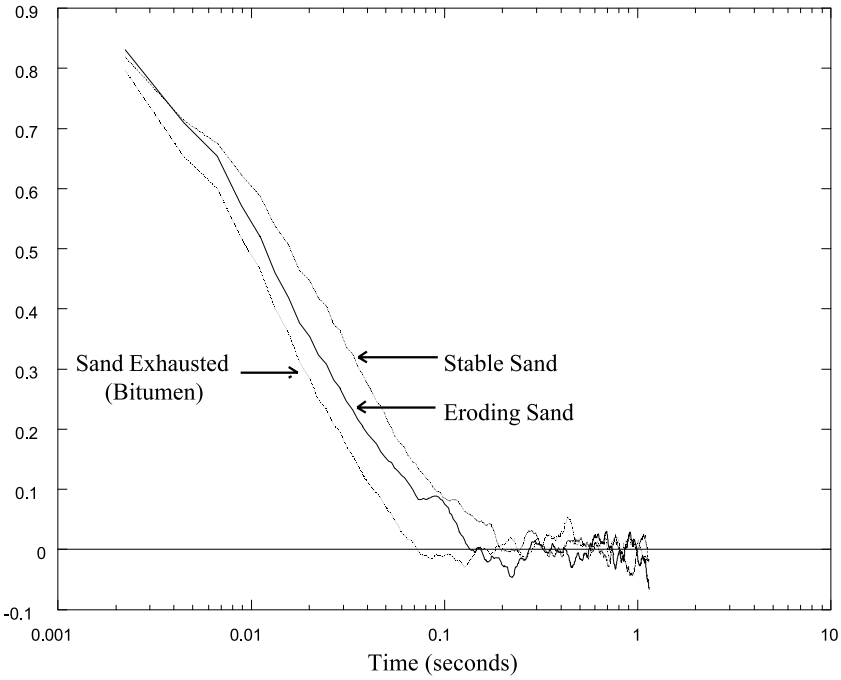

Figure 7. Autocorrelations, Murdoch Turbulence Probe in AWA wind-tunnel. Measurements were taken over the Stable Sand surface with the engine speed set at 800 rpm, below the threshold for erosion. The other curves were with engine speed set at 1600 rpm.

In fitting the velocity profiles during erosion, the displacement must increase during the erosion process. Hence the profile analysis considered two values of the displacement distance d, d = 5 mm and d = 0 mm. d = 5 mm was preferred because the profile during erosion was similar to the profile over the Peg-board. The coefficient of determination r^2 exceeded 0.99 for all the profiles and was not sensitive to the selection of d.

Accounting for d, values for κ between the Stable Sand, Transport Limited case and the Bitumen are similar to the Peg-board at $P_{0.05}$ (Table III). Also, z_0 for the Transport Limited case (d = 5) is similar in magnitude to that observed for the Peg-board with t = 0.66 (equation 18, parameters from Table III). However, while κ over the bitumen surface (0.34) is within the range of recorded values (0.26 to 0.35), it is significantly different from κ over the Peg-board (P <0.001). With d = 0, κ is about 0.26, a low value.

As with both the Peg-board and the bitumen surface, the erosion profiles appear 'logarithmic' almost to the tunnel ceiling (Figure 8). The velocities measured over the bare bitumen after the sand has blown away are a little higher; this probably indicates leakage around the 'skirts' of the tunnel; sand remains to 'seal' the tunnel edges and the skirts after the sand has been eroded from the bitumen surface. There

Table III. Profile parameters for blowing sand estimated with a rake of pitot and static tubes. δ is the boundary-layer height; MTP u_*, friction velocity estimate from the MTP; U_δ, velocity at height δ; N, the number of heights the velocity was sampled; κ, the von Kármán constant obtained form the log profile; z_0, the roughness length. The standard error for the profile statistics comes from equations 15, 16 and 17. The null hypothesis H_0 is that measured κ values are equal to the 'Peg-board' values ($\kappa = \kappa_{\text{peg}}$), using a t-test (equation 18). All the profiles are for an engine speed of 1600 rpm except the Stable Sand, which was at 800 rpm.

Surface	δ	U_δ	MTP u_*	N	κ	$t_{(0.05)}$	z_0	Standard error for			r^2
	mm	m/s	m/s			$\kappa = \kappa_{\text{peg}}$	mm	κ	z_0	$\ln(z_0)$	
Erosion studies											
Stable Sand	53	5.33	0.21	6	0.35	not significant	0.008	0.03	0.003	0.444	0.978
Transport limited											
$d = 0$ mm	238	13.05	0.64	12	0.26	significant @ 0.001 level	1.3	0.01	0.115	0.089	0.996
$d = 5$ mm	238	13.05	0.64	12	0.29	not significant	0.710	0.01	0.090	0.126	0.991
Supply limited	sand exhausted (only bitumen)										
	58	10.58	0.39								
Preliminary tests											
Bitumen	63	10.95	0.49	6	0.34	significant @ 0.01 level	0.032	0.01	0.005	0.163	0.997
'Peg-board'	303	12.88	0.64	11	0.30	0.01 not applicable	0.641	0.01	0.054	0.085	0.995

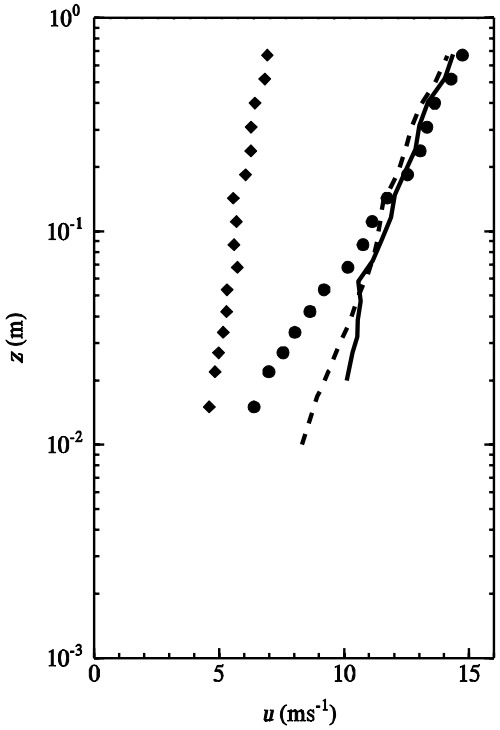

Figure 8. Profiles over sand and bitumen surfaces, measured with the pitot rake. ♦ Stable Sand surface below threshold for erosion. ● Transport Limited case. ——— Sand Exhausted exposing the bitumen surface. – – – – Preliminary tests over a bitumen surface.

is also the tendency for any remaining sand to fill in low spots in the surface, perhaps making the bitumen surface smoother.

Profiles in the Transport Limited case (Figure 8) is slightly convex to the origin close to the surface (the 'kink') and less regular over the entire profile. Note that as erosion proceeds (Sand Exhausted) the lower portion of the profile is more distorted. The distortion that appears in the profile during erosion is not only a response to saltating particles, but also a response to the lower pitot tubes being blocked. Continuation of the experiment as the erosion becomes Supply Limited brings higher wind speeds near the surface but there is little response because the tubes are blocked; dynamic pressures measured near the surface remain low and velocities tend to be underestimated.

The stress measurements with the Murdoch Turbulence Probe over the Stable Sand surface and the bitumen surfaces (including Sand Exhausted) were near the estimated height of the boundary-layer where the stress is expected to be close to zero. Yet we recorded Reynolds stresses between 0.044 m^2/s^2 and 0.24 m^2/s^2, well above zero. This inconsistency will be discussed in Section 8. It is noteworthy that

stress measurements and corresponding friction velocities are similar to friction velocities derived from profile parameters over both the rough surface (Peg-board) and the eroding surfaces.

Both the threshold friction velocity (u_{*t}) and the roughness length (z_0) of the sand are in close agreement with Bagnold's predictions for a sand with a mean diameter D of 210 μm (Table I). The threshold friction velocity was just above 0.21 m/s. The calculated threshold is 0.20 m/s from Bagnold's formula,

$$u_{*t} = A\sqrt{\frac{\varphi - \rho}{\rho} g D} \quad \text{for} \quad D > 0.0002 \text{ m} \tag{19}$$

with φ the grain density (2650 kg/m^3 for quartz), ρ the fluid density (1.2 kg/m^3 for air) and g the acceleration of gravity (9.8 m/s) with the empirical coefficient A equal to 0.1. Similarly, Bagnold suggested that the roughness length is D/30. This corresponds to 0.007 mm compared with a value estimated from the log profile of 0.008 mm; however, the 95% confidence limits in this value are poor, $\pm$ 0.009 mm.

8. Discussion

The constant stress or the 'inner-layer', over which the Law of the Wall, Equation (1), applies is expected to extend from about 2 to 5 times the height of the roughness elements to about 10% to 20% of δ. In the atmosphere, because of the depth of the boundary-layer ($\sim$100 to 1000 m), the region over which the Law of the Wall applies is usually many metres deep; this is much greater than the height of the saltation cloud, which is only centimetres deep. In most wind-tunnels the saltation cloud is relatively deep and the BL is shallow, because of fetch and tunnel height constraints. Here, a tripping fence at the approach to the working section is used to 'hasten' the development of the BL. Nevertheless, an 'inner-layer' of 10% of the BL in the AWA tunnel corresponds to only 0.006 m of height for a 'smooth surface (sand or bitumen) to 0.030 m of height for 'rough' surfaces (the Peg-board or during eroding conditions). Therefore, the logarithmic velocity profile observed in the AWA tunnel may best be described as the 'outer-layer' of the BL and it is unlikely that Equation (1) applies.

Owen and Gillette (1985) suggested that the Wake Law should be used to describe the velocity profile of the 'outer' layer and estimate the surface shear where the BL is shallow. Spies *et al*. (1995) applied Coles' (1956) wake law to eroding sand. Similarly, Daily and Harleman (1966) used the data of others (Freeman, 1932; Klebanoff and Diehl, 1952; Schultz-Grunow, 1940; Moore, 1951) to support their argument that the velocity profile of the outer region was described by a Log Defect Law; this is an expression like (1) and has a constant similar to the von Kármán constant but equal to 0.267. Accepting that the logarithmic profile (1) does not apply, a Wake Law (Coles, 1956) or a Defect Law (Daily and Harleman, 1966) should apply. We suggest that a Defect Law like (1) but with κ about 0.3 best describe the observations.

Estimates of κ are in accord with those in similar tunnels. Raupach and Leys (1990) observed that $\kappa = 0.29$ for a tent shaped tunnel of design identical to the AWA tunnel; $\kappa = 0.35$ for a similar, rectangular tunnel. Values for the von Kármán constant of about 0.3, are comparable with those obtained by Daily and Harleman (1966), and lower than the commonly accepted value for atmospheric profiles, 0.4.

Presuming that a wake or velocity defect law applies, and the probe measurements are at 0.05 m, stresses are measured above the height of the 'inner' layer where (1) applies and above the region where stresses are commonly considered constant. It is unlikely that the Reynolds stresses are wrong or that they underestimate the surface shear stress, which would also result in a lower κ. Firstly, measurements from the probe agree with a X-wire probe (for $\overline{u'w'}$, $r = 0.962$) when calibrated in a clean environment (Smith, 1994). Secondly, we obtain threshold friction velocities over the stable sand similar to predicted values, consistent with the probe providing reliable estimates of the surface stress. We suggest that the constant stress layer may be much deeper than the 'inner layer' and the velocity profile may not be a good surrogate for the Reynolds stress profile. Data of Raupach *et al*. (1980) show that while Equation (1) applies to the lower 20% of the BL (Raupach *et al*., 1980, Figure 4), stresses remain nearly constant well above the height of the 'inner' layer to about 30% of BL (Raupach *et al*., 1980, Figure 8). Consequently, the probe placed at 0.05 m over a rough surface is about 30% into the BL.

However, recognising that the probe over the 'Stable Sand' and 'Bitumen' surfaces is near the top of the BL, the Reynolds stress should be near to zero. Over the 'Stable Sand' with $\delta = 0.053$ m, a significant stress is measured (0.044 m^2/s^2). It seems that δ has been underestimated and that the inconsistency merely reflects the difficulty in determining δ. Estimating the height of the boundary-layer using similarity considerations is imprecise, especially for 'smooth' surfaces, with small 'boundary' layer heights. In the AWA tunnel for these smooth surfaces, δ is about 0.2 of the value for rough surfaces (Peg-boards and eroding sand). Other studies have not shown such a large variation in δ with surface roughness. For example, Lyles *et al*. (1971) report a much deeper BL relative to their rough surface; $\delta = 0.241$ m over a smooth surface and $\delta = 0.295$ m over a surface covered with 0.016 m diameter spheres, a ratio of 0.82. Similarly, Raupach *et al*. (1980) report $\delta = 0.053$ m over a smooth surface and $\delta = 0.012$ m over surface E, a ratio of 0.44. Considering these ratios, it is likely that δ for the 'Stable Sand' and 'Bitumen' surface is around 0.20 m and the probe is marginally within the constant stress layer and producing an estimate of the surface stress.

With erosion, Figure 6 and Tables II and III show that u_* decreases from 0.64 m/s for the Transport Limited case, to 0.49 m/s when erosion is Supply Limited, and 0.39 m/s over a bare surface (bitumen). This is contrary to Bagnold, who suggested that the stress remains constant. However, Bagnold inferred the stress from the profile and had an all-eroding surface. It is apparent that in wind-tunnels during erosion the surface stress is modified by the soil flux rate. This is very likely

the case in the atmosphere as well. To compare the ability of different surfaces to control erosion it is necessary to ensure that surfaces are subject to the same wind, the 'overriding' wind. A scale parameter(s) is required to characterise this 'overriding' wind, particularly for extrapolations of wind-tunnel results into field conditions. The scale is not necessarily the friction velocity.

Instruments placed in the tunnel do alter the wind properties; supports for the pitot-static rake and associated tubing are significant; the sensor part of the turbulence probe is designed to minimise obstruction. Also, there are pressure gradients along the tunnel and these are affected by instruments placed near the end of the tunnel. Such effects are present in the data from all wind-tunnels and become more significant at higher wind speeds in small portable tunnels. The effect must be minimised; single instruments, such as the probe, may best serve this purpose.

An objective of this work is to achieve an instrument that provides scaling parameters during erosion at the point of measurement. These may be the friction velocity and the integral length scale as measured by the Murdoch Turbulence Probe, or some other statistical properties. In any case we must characterise the 'overriding' wind. A suitable scale might be the free stream velocity or the velocity at the top of the boundary-layer. In the atmosphere the wind profile develops from the surface upwards; such a reference wind speed should remain unaffected by changes at the surface. In a wind-tunnel there is no 'freestream velocity'; the overall dimension is comparable to the depth of the BL and the centre of the tunnel tends to be a convergent part of the lower and upper boundary-layers.

Presuming one scale is the friction velocity, a companion scale might be expected to be independent of the Reynolds stress. Consider that $\overline{u'u'}$, T or Λ may be suitable as such a scale. In Table II, the turbulence $\overline{u'u'}$ during erosion was proportional to the stress (10 times $-\overline{u'w'}$) over a range of engine speeds and conditions (Figure 6 and Table II) and so is not independent of the Reynolds stress. The integral time scale T varies from 0.04 s over Stable Sand to 0.017 s when the sand is exhausted. The integral length scale Λ doesn't change much with either erosion, wind speed or Reynolds stress and may be a measure of the scale (or relative vertical measurement) in the wind-tunnel.

9. Conclusions

The Murdoch Turbulence Probe works well in harsh flows providing estimates of velocity u and turbulence statistics including $\overline{u'w'}$, $\overline{u'u'}$, T and Λ. Turbulence intensity is in close agreement with values in the literature but the ratio of the turbulence to the friction velocity is at the high end of the range. Measurements of the Reynolds stress agree with predictions of the surface stress based on either threshold friction velocity or a 'logarithmic' profile with $\kappa = 0.3$.

If u_* is the only scale that is required to define erosion, then the Probe can be used to replace profile techniques and can directly estimate the surface stress. As

erosion occurs, however, the shear increases. With a lack of a supply of sand, with Supply Limited conditions (see footnote 3), the shear decreases.

Bagnold performed experiments normalised with stress values at lower levels, within the 'constant stress' zone of the profile. One of his important results was that these stress values, or their u_* equivalents, remained the same both with and without erosion. However, the 'overriding' wind was adjusted to achieve predetermined surface shear stress values. Bagnold would have changed the fan speed in his tunnel and used wind profiles in the field that corresponded to predetermined constant stress conditions, simply to normalise his experiments.

It is probable that a measure of the 'overriding' wind needs to be included, particularly to extend wind-tunnel experiments out and into the field. This contrasts with existing practice of comparing soil flux rate of soils of different types and treatments at the same u_*. It is to be determined if an appropriate measure of the 'overriding' wind can be determined from the Murdoch Turbulence Probe, or with any single instrument.

Velocity profiles during erosion of a sand surface in the AWA tunnel are similar to profiles over stable rough surfaces. A logarithmic law provides a good estimate of u_* and z_0 with $\kappa \cong 0.3$. However, estimates of κ of about 0.3 are much lower than the commonly accepted value of 0.4. We suggest that the 'inner layer' of the wind speed profile has not developed sufficiently for the log law to produce appropriate values of u_*. The observed profile appears to be an 'outer layer' of the BL which may best be described by a 'Wake Law' or 'Defect Law'.

Over smooth surfaces, Reynolds stress measurements near the top of the BL were consistent with estimates of surface stress. This contrasts with the expectation of a small shear stress. This anomaly possibly reflects an inability to accurately define the extent of the boundary-layer. Even with equilibrium flow over a smooth surface the wind speed profile may not reflect the Reynolds stress profile.

Acknowledgements

Stewart Smith was supported by APRA (Australian Commonwealth Government) scholarship. Significant financial support was provided by Murdoch University, Agriculture Western Australia, NSCP and LWRDDC. The authors thank Roger Handsworth (Platypus Engineering, Hobart) who was responsible for much of the mechanical design and manufacture of the probe and Teik Oh for the analog interface to the DSP hardware. John Tubb and Chris Horgan (Curtin University, Mechanical Engineering) and Dr Dan Carter (Agriculture WA) for support, advice and assistance during various stages of the project. Thanks also go to Mr Rob Hetherington (Agriculture WA) for his assistance with the probe tests, and the design, construction and operation of the Agriculture Western Australia portable wind-tunnel and pitot rake.

References

R.A. Bagnold, *The Physics of Blown Sand and Desert Dunes*. Methuen, London (1941).

H.A. Becker and A.P.G. Brown, Response of pitot probes in turbulent streams. *J. Fluid Mech*. **62** (1974) 85–114.

H. Bergh and H. Tijdeman, *Theoretical and Experimental Results for the Dynamic Response of Pressure Measuring Systems*. National Aero- and Astronautical Research Institute, Amsterdam, Report NLR-TRF, 238 (1965) 19 pp.

T. Brancatisano, D. Carter, J. Hopwood, M. Raupach, W.D. Scott, S.E. Smith and J. Tubb, *Erosion Wind Tunnel Workshop*. Environmental Science Report 92/8, Murdoch University, Australia (1991).

D.W. Bryer and R.C. Pankhurst, *Pressure Probe Methods for Determining Wind Speed and Flow Direction*, National Physical Laboratory, Her Majesty's Stationary Office, pp. 16, 57, 68 (1971).

D. Coles, The law of the wake in the turbulent boundary layer. *J. Fluid Mech*. **1** (1956) 191–226.

J.W. Daily and D.R.F. Harleman, *Fluid Dynamics*. Addison-Wesley Publishing Company, Reading, Massachusetts (1966).

H.B. Freeman *Force measurements on a 1/40-Scale Model of the US Air-Ship Akron*. Nat. Advisory Comm. Aeron., Report 432 (1932).

R. Greeley and J.D. Iversen, *Wind as a Geological Process on Earth, Mars, Venus and Titan*. Cambridge University Press, Cambridge (1985).

S.J. Gumley, Tubing systems for pneumatic averaging of fluctuating pressures. *J. Wind Engineering and Industrial Aerodynamics* **12** (1983) 189–228.

J.D. Holmes and R.E. Lewis, The dynamic response of pressure-measurement systems. In: 9th AFMC, Australasian Fluid Mechanics Conference, Auckland, New Zealand 8–12 December 1986, University of Auckland, Auckland (1986) pp. 537–540.

J.D. Holmes and R.E. Lewis, Optimization of dynamic pressure-measurement Systems. I. Single point measurements. *J. Wind Engineering and Industrial Aerodynamics* **25** (1987a) 249–273.

J.D. Holmes and R.E. Lewis, Optimization of dynamic pressure-measurement systems. II. Parallel tube-manifold systems. *J. Wind Engineering and Industrial Aerodynamics* **25** (1987b) 275–290.

A.S. Iberall, Attenuation of oscillating pressures in instrument lines. *J. Research of the National Bureau of Standards* **45** (1950) 85–108.

H.P.A.H. Irwin, K.R. Cooper and R. Gerard, Correction of distortion effects caused by tubing systems. *J. Industrial Aerodynamics* **5** (1979) 93–107.

P.S. Klebanoff and Z.W. Diehl, *Some Features of an Artificially Thickened Fully Developed Turbulent Boundary Layers with Zero-Pressure Gradient*. Nat. Advisory Comm. Aeron., Rept 1110 (1952).

J.F. Leys, The threshold friction velocities and soil flux rates of selected soils in south-west New South Wales, Australia. In: O.E. Barndorff-Nielsen and B.B. Willetts (Eds.), *Aeolian grain transport (2): The erosional environment*. Acta-Mechanica-Supplementum, 1991, No 2. pp. 103–112.

J. Leys, T. Koen and G. McTainsh, The effect of dry aggregation and percentage clay on sediment flux as measured by a portable field wind tunnel. *Aust. J. Soil Res*. **34(6)** (1996) 849–861.

L. Lyles, L.A. Disrud and K. Krauss, Turbulence intensity as influenced by surface roughness and mean velocity in a wind tunnel boundary layer. *Trans. ASAE*. **14** (1971) 285–289.

C. McKenna-Neuman and W.G. Nickling, Momentum extraction with saltation: Implications for experimental evaluation of wind profile parameters. *Boundary-Layer Meteorol*. **68** (1994) 35–50.

W.F. Moore, *An Experimental Investigation of the Boundary Layer Development Along a Rough Surface*. Ph.D. Thesis, State University of Iowa (1951).

P. Owen and D. Gillette, Wind tunnel constraint on saltation. In: O.E. Barndorff-Nielson, J.T. Moller, K. Rasmussen and B.B. Willetts (Eds.), *Proceedings of the International Workshop on the Physics of Blown Sands*, Memoirs No 8, vol 2, Department of Theoretical Statistics, Inst. Mathematics, Aarhus (1985) pp. 253–269.

E. Ower and R.C. Pankhurst, *The measurement of air flow*, 4th ed., revised. Pergamon Press Ltd, Oxford, London, p. 56 (1966).

M.R. Raupach, Drag partition on rough surfaces. *Boundary-Layer Meteorol*. **60** (1992) 375–395.

M.R. Raupach and J.F. Leys, Aerodynamics of a portable wind tunnel for measuring soil erodibility by wind. *Aust. J. Soil Res*. **28** (1990) 177–191.

M.R. Raupach, A.S. Thom and I. Edwards, A wind tunnel study of turbulent flow close to regularly arrayed rough surfaces. *Boundary-Layer Meteorol*. **18** (1980) 373–397

M.R. Raupach, R.A. Antonia and S. Rajagopalan, *Rough-wall turbulent boundary layers*. Applied Mechanical Reviews. 44 (1), ASME Book No AMR084 (1991) pp. 1–25.

F. Schultz-Grunow, Neues Widerstandsgesetz für glatte Platten. Luftfahrtforschung. 17, 239 (Also Nat. Advisory Comm. Aeron., Tech. Memo. 986, 1941) (1940).

W.D. Scott, *Turbulence: Rotating Statistics*, Section 5.6 in Maple for Environmental Sciences: a Helping Hand, Springer-Verlag, 406 pp. (2001) ISBN 3-540-65826-2.

W.D. Scott and D.J. Carter, The logarithmic profile in wind erosion: an algebraic solution. *Boundary-Layer Meteorol*. **34** (1986) 303–310.

W.D. Scott and J. Tubb, An assessment of agricultural wind tunnels. In: Agricultural Engineering Conference: Toowoomba 11-14 November 1990: preprints of papers/sponsored by National Committee on Agricultural Engineering, The Institution of Engineers Australia; co-sponsored by American Society of Agricultural Engineers. Institution of Engineers Australia, Barton, A.C.T. (1990) pp. 138–146.

W.D. Scott, J.M. Hopwood and K.J. Summers, A mathematical model of suspension with saltation. *Acta Mechanica* **108** (1995) 1–22.

W.D. Scott, C. Twomey, L. Butcher and J. Kerr, *The Murdoch Turbulence Probe* (19 min VHS or PAL Video), prepared by the Academic Services Unit, Murdoch University (1993).

Y. Shao, G.H. McTainsh, J.F. Leys and M.R. Raupach, Efficiencies of sediment samplers for wind erosion measurement. *Aust. J. Soil Res*. **31(4)** (1993) 519–532.

S.E. Smith, *An Instrument to Measure Turbulence During Wind Erosion*. Ph.D. Thesis, Murdoch University, Western Australia (1994).

P. Spies, I.K. McEwan and G.R. Butterfield, On wind velocity profiles taken in wind tunnels with saltation. *Sedimentology* **42** (1995) 515–521.

R.B. Stull, *An Introduction to Boundary Layer Meteorology*. Kluwer Academic Publishers, Dordrecht (1988).

M.L. Wesley, C.B. Tanner and G.W. Thurtell, An improved pressure-sphere anemometer. *Boundary-Layer Meteorol*. **2** (1972) 275–283.

R.H. Wilkinson, A method for evaluating statistical errors associated with logarithmic velocity profiles. *Geo-Marine Letters* **3** (1984) 49–52.

A.W. Zingg and N.P. Woodruff, Calibration of a portable wind tunnel for the simple determination of roughness and drag on field surfaces. *Agron. J*. **43** (1951) 189–193.